

ND-A153 737

THERMAL STABILITY OF STATIC CORONAL LOOPS I EFFECTS OF  
BOUNDARY CONDITION. (U) STANFORD UNIV CA CENTER FOR  
SPACE SCIENCE AND ASTROPHYSICS S K ANTIOCHOS ET AL.

1/1

UNCLASSIFIED

MAR 85 CSSA-ASTRO-85-14 N00014-85-K-0111

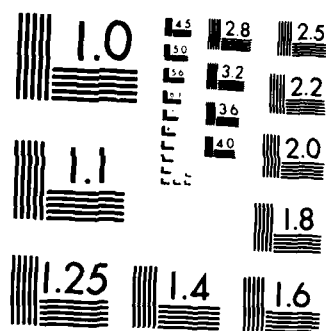
F/G 3/2

NL

END

FILMED

DTIC



MICROCOPY RESOLUTION TEST CHART  
NATIONAL BUREAU OF STANDARDS-1963 A

2

# C S S A

AD-A153 737

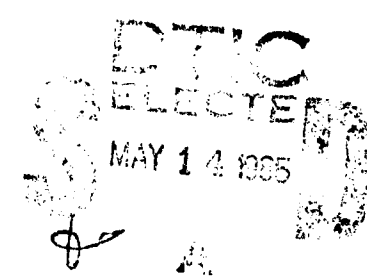
## THERMAL STABILITY OF STATIC CORONAL LOOPS: I. EFFECTS OF BOUNDARY CONDITIONS

S. K. Antiochos and E. C. Shoub  
Center for Space Science and Astrophysics  
Stanford University

C.-H. An\*  
Center for Astrophysics and Space Science  
University of California-San Diego

A. G. Emslie  
Department of Physics  
University of Alabama

CSSA-ASTRO-85-14  
March 1985



**CENTER FOR SPACE SCIENCE AND ASTROPHYSICS**  
**STANFORD UNIVERSITY**  
**Stanford, California**

This document has been approved  
for public release and sale; its  
distribution is unlimited

35 4 04 010

**THERMAL STABILITY OF STATIC CORONAL LOOPS:  
I. EFFECTS OF BOUNDARY CONDITIONS**

**S. K. Antiochos and E. C. Shoub**  
Center for Space Science and Astrophysics  
Stanford University

**C.-H. An\***  
Center for Astrophysics and Space Science  
University of California-San Diego

**A. G. Emslie**  
Department of Physics  
University of Alabama

**CSSA-ASTRO-85-14**  
March 1985

**NATIONAL AERONAUTICS AND SPACE ADMINISTRATION**  
Grant NGL 05-020-272  
Grant NAGW-92  
Grant NGR 05-020-668

**OFFICE OF NAVAL RESEARCH**  
Contract N00014-85-K-0111

\*Current address: NASA-Marshall Space Flight Center

11  
12  
13  
14  
15  
16  
17  
18  
19  
20  
21  
22  
23  
24  
25  
26  
27  
28  
29  
30  
31  
32  
33  
34  
35  
36  
37  
38  
39  
40  
41  
42  
43  
44  
45  
46  
47  
48  
49  
50  
51  
52  
53  
54  
55  
56  
57  
58  
59  
60  
61  
62  
63  
64  
65  
66  
67  
68  
69  
70  
71  
72  
73  
74  
75  
76  
77  
78  
79  
80  
81  
82  
83  
84  
85  
86  
87  
88  
89  
90  
91  
92  
93  
94  
95  
96  
97  
98  
99  
100  
101  
102  
103  
104  
105  
106  
107  
108  
109  
110  
111  
112  
113  
114  
115  
116  
117  
118  
119  
120  
121  
122  
123  
124  
125  
126  
127  
128  
129  
130  
131  
132  
133  
134  
135  
136  
137  
138  
139  
140  
141  
142  
143  
144  
145  
146  
147  
148  
149  
150  
151  
152  
153  
154  
155  
156  
157  
158  
159  
160  
161  
162  
163  
164  
165  
166  
167  
168  
169  
170  
171  
172  
173  
174  
175  
176  
177  
178  
179  
180  
181  
182  
183  
184  
185  
186  
187  
188  
189  
190  
191  
192  
193  
194  
195  
196  
197  
198  
199  
200  
201  
202  
203  
204  
205  
206  
207  
208  
209  
210  
211  
212  
213  
214  
215  
216  
217  
218  
219  
220  
221  
222  
223  
224  
225  
226  
227  
228  
229  
230  
231  
232  
233  
234  
235  
236  
237  
238  
239  
240  
241  
242  
243  
244  
245  
246  
247  
248  
249  
250  
251  
252  
253  
254  
255  
256  
257  
258  
259  
260  
261  
262  
263  
264  
265  
266  
267  
268  
269  
270  
271  
272  
273  
274  
275  
276  
277  
278  
279  
280  
281  
282  
283  
284  
285  
286  
287  
288  
289  
290  
291  
292  
293  
294  
295  
296  
297  
298  
299  
300  
301  
302  
303  
304  
305  
306  
307  
308  
309  
310  
311  
312  
313  
314  
315  
316  
317  
318  
319  
320  
321  
322  
323  
324  
325  
326  
327  
328  
329  
330  
331  
332  
333  
334  
335  
336  
337  
338  
339  
340  
341  
342  
343  
344  
345  
346  
347  
348  
349  
350  
351  
352  
353  
354  
355  
356  
357  
358  
359  
360  
361  
362  
363  
364  
365  
366  
367  
368  
369  
370  
371  
372  
373  
374  
375  
376  
377  
378  
379  
380  
381  
382  
383  
384  
385  
386  
387  
388  
389  
390  
391  
392  
393  
394  
395  
396  
397  
398  
399  
400  
401  
402  
403  
404  
405  
406  
407  
408  
409  
410  
411  
412  
413  
414  
415  
416  
417  
418  
419  
420  
421  
422  
423  
424  
425  
426  
427  
428  
429  
430  
431  
432  
433  
434  
435  
436  
437  
438  
439  
440  
441  
442  
443  
444  
445  
446  
447  
448  
449  
450  
451  
452  
453  
454  
455  
456  
457  
458  
459  
460  
461  
462  
463  
464  
465  
466  
467  
468  
469  
470  
471  
472  
473  
474  
475  
476  
477  
478  
479  
480  
481  
482  
483  
484  
485  
486  
487  
488  
489  
490  
491  
492  
493  
494  
495  
496  
497  
498  
499  
500  
501  
502  
503  
504  
505  
506  
507  
508  
509  
510  
511  
512  
513  
514  
515  
516  
517  
518  
519  
520  
521  
522  
523  
524  
525  
526  
527  
528  
529  
530  
531  
532  
533  
534  
535  
536  
537  
538  
539  
540  
541  
542  
543  
544  
545  
546  
547  
548  
549  
550  
551  
552  
553  
554  
555  
556  
557  
558  
559  
560  
561  
562  
563  
564  
565  
566  
567  
568  
569  
570  
571  
572  
573  
574  
575  
576  
577  
578  
579  
580  
581  
582  
583  
584  
585  
586  
587  
588  
589  
590  
591  
592  
593  
594  
595  
596  
597  
598  
599  
600  
601  
602  
603  
604  
605  
606  
607  
608  
609  
610  
611  
612  
613  
614  
615  
616  
617  
618  
619  
620  
621  
622  
623  
624  
625  
626  
627  
628  
629  
630  
631  
632  
633  
634  
635  
636  
637  
638  
639  
640  
641  
642  
643  
644  
645  
646  
647  
648  
649  
650  
651  
652  
653  
654  
655  
656  
657  
658  
659  
660  
661  
662  
663  
664  
665  
666  
667  
668  
669  
670  
671  
672  
673  
674  
675  
676  
677  
678  
679  
680  
681  
682  
683  
684  
685  
686  
687  
688  
689  
690  
691  
692  
693  
694  
695  
696  
697  
698  
699  
700  
701  
702  
703  
704  
705  
706  
707  
708  
709  
710  
711  
712  
713  
714  
715  
716  
717  
718  
719  
720  
721  
722  
723  
724  
725  
726  
727  
728  
729  
730  
731  
732  
733  
734  
735  
736  
737  
738  
739  
740  
741  
742  
743  
744  
745  
746  
747  
748  
749  
750  
751  
752  
753  
754  
755  
756  
757  
758  
759  
760  
761  
762  
763  
764  
765  
766  
767  
768  
769  
770  
771  
772  
773  
774  
775  
776  
777  
778  
779  
780  
781  
782  
783  
784  
785  
786  
787  
788  
789  
790  
791  
792  
793  
794  
795  
796  
797  
798  
799  
800  
801  
802  
803  
804  
805  
806  
807  
808  
809  
810  
811  
812  
813  
814  
815  
816  
817  
818  
819  
820  
821  
822  
823  
824  
825  
826  
827  
828  
829  
830  
831  
832  
833  
834  
835  
836  
837  
838  
839  
840  
841  
842  
843  
844  
845  
846  
847  
848  
849  
850  
851  
852  
853  
854  
855  
856  
857  
858  
859  
860  
861  
862  
863  
864  
865  
866  
867  
868  
869  
870  
871  
872  
873  
874  
875  
876  
877  
878  
879  
880  
881  
882  
883  
884  
885  
886  
887  
888  
889  
890  
891  
892  
893  
894  
895  
896  
897  
898  
899  
900  
901  
902  
903  
904  
905  
906  
907  
908  
909  
910  
911  
912  
913  
914  
915  
916  
917  
918  
919  
920  
921  
922  
923  
924  
925  
926  
927  
928  
929  
930  
931  
932  
933  
934  
935  
936  
937  
938  
939  
940  
941  
942  
943  
944  
945  
946  
947  
948  
949  
950  
951  
952  
953  
954  
955  
956  
957  
958  
959  
960  
961  
962  
963  
964  
965  
966  
967  
968  
969  
970  
971  
972  
973  
974  
975  
976  
977  
978  
979  
980  
981  
982  
983  
984  
985  
986  
987  
988  
989  
990  
991  
992  
993  
994  
995  
996  
997  
998  
999  
1000  
1001  
1002  
1003  
1004  
1005  
1006  
1007  
1008  
1009  
1010  
1011  
1012  
1013  
1014  
1015  
1016  
1017  
1018  
1019  
1020  
1021  
1022  
1023  
1024  
1025  
1026  
1027  
1028  
1029  
1030  
1031  
1032  
1033  
1034  
1035  
1036  
1037  
1038  
1039  
1040  
1041  
1042  
1043  
1044  
1045  
1046  
1047  
1048  
1049  
1050  
1051  
1052  
1053  
1054  
1055  
1056  
1057  
1058  
1059  
1060  
1061  
1062  
1063  
1064  
1065  
1066  
1067  
1068  
1069  
1070  
1071  
1072  
1073  
1074  
1075  
1076  
1077  
1078  
1079  
1080  
1081  
1082  
1083  
1084  
1085  
1086  
1087  
1088  
1089  
1090  
1091  
1092  
1093  
1094  
1095  
1096  
1097  
1098  
1099  
1100  
1101  
1102  
1103  
1104  
1105  
1106  
1107  
1108  
1109  
1110  
1111  
1112  
1113  
1114  
1115  
1116  
1117  
1118  
1119  
1120  
1121  
1122  
1123  
1124  
1125  
1126  
1127  
1128  
1129  
1130  
1131  
1132  
1133  
1134  
1135  
1136  
1137  
1138  
1139  
1140  
1141  
1142  
1143  
1144  
1145  
1146  
1147  
1148  
1149  
1150  
1151  
1152  
1153  
1154  
1155  
1156  
1157  
1158  
1159  
1160  
1161  
1162  
1163  
1164  
1165  
1166  
1167  
1168  
1169  
1170  
1171  
1172  
1173  
1174  
1175  
1176  
1177  
1178  
1179  
1180  
1181  
1182  
1183  
1184  
1185  
1186  
1187  
1188  
1189  
1190  
1191  
1192  
1193  
1194  
1195  
1196  
1197  
1198  
1199  
1200  
1201  
1202  
1203  
1204  
1205  
1206  
1207  
1208  
1209  
1210  
1211  
1212  
1213  
1214  
1215  
1216  
1217  
1218  
1219  
1220  
1221  
1222  
1223  
1224  
1225  
1226  
1227  
1228  
1229  
1230  
1231  
1232  
1233  
1234  
1235  
1236  
1237  
1238  
1239  
1240  
1241  
1242  
1243  
1244  
1245  
1246  
1247  
1248  
1249  
1250  
1251  
1252  
1253  
1254  
1255  
1256  
1257  
1258  
1259  
1260  
1261  
1262  
1263  
1264  
1265  
1266  
1267  
1268  
1269  
1270  
1271  
1272  
1273  
1274  
1275  
1276  
1277  
1278  
1279  
1280  
1281  
1282  
1283  
1284  
1285  
1286  
1287  
1288  
1289  
1290  
1291  
1292  
1293  
1294  
1295  
1296  
1297  
1298  
1299  
1300  
1301  
1302  
1303  
1304  
1305  
1306  
1307  
1308  
1309  
1310  
1311  
1312  
1313  
1314  
1315  
1316  
1317  
1318  
1319  
1320  
1321  
1322  
1323  
1324  
1325  
1326  
1327  
1328  
1329  
1330  
1331  
1332  
1333  
1334  
1335  
1336  
1337  
1338  
1339  
1340  
1341  
1342  
1343  
1344  
1345  
1346  
1347  
1348  
1349  
1350  
1351  
1352  
1353  
1354  
1355  
1356  
1357  
1358  
1359  
1360  
1361  
1362  
1363  
1364  
1365  
1366  
1367  
1368  
1369  
1370  
1371  
1372  
1373  
1374  
1375  
1376  
1377  
1378  
1379  
1380  
1381  
1382  
1383  
1384  
1385  
1386  
1387  
1388  
1389  
1390  
1391  
1392  
1393  
1394  
1395  
1396  
1397  
1398  
1399  
1400  
1401  
1402  
1403  
1404  
1405  
1406  
1407  
1408  
1409  
1410  
1411  
1412  
1413  
1414  
1415  
1416  
1417  
1418  
1419  
1420  
1421  
1422  
1423  
1424  
1425  
1426  
1427  
1428  
1429  
1430  
1431  
1432  
1433  
1434  
1435  
1436  
1437  
1438  
1439  
1440  
1441  
1442  
1443  
1444  
1445  
1446  
1447  
1448  
1449  
1450  
1451  
1452  
1453  
1454  
1455  
1456  
1457  
1458  
1459  
1460  
1461  
1462  
1463  
1464  
1465  
1466  
1467  
1468  
1469  
1470  
1471  
1472  
1473  
1474  
1475  
1476  
1477  
1478  
1479  
1480  
1481  
1482  
1483  
1484  
1485  
1486  
1487  
1488  
1489  
1490  
1491  
1492  
1493  
1494  
1495  
1496  
1497  
1498  
1499  
1500  
1501  
1502  
1503  
1504  
1505  
1506  
1507  
1508  
1509  
1510  
1511  
1512  
1513  
1514  
1515  
1516  
1517  
1518  
1519  
1520  
1521  
1522  
1523  
1524  
1525  
1526  
1527  
1528  
1529  
1530  
1531  
1532  
1533  
1534  
1535  
1536  
1537  
1538  
1539  
1540  
1541  
1542  
1543  
1544  
1545  
1546  
1547  
1548  
1549  
1550  
1551  
1552  
1553  
1554  
1555  
1556  
1557  
1558  
1559  
1560  
1561  
1562  
1563  
1564  
1565  
1566  
1567  
1568  
1569  
1570  
1571  
1572  
1573  
1574  
1575  
1576  
1577  
1578  
1579  
1580  
1581  
1582  
1583  
1584  
1585  
1586  
1587  
1588  
1589  
1590  
1591  
1592  
1593  
1594  
1595  
1596  
1597  
1598  
1599  
1600  
1601  
1602  
1603  
1604  
1605  
1606  
1607  
1608  
1609  
1610  
1611  
1612  
1613  
1614  
1615  
1616  
1617  
1618  
1619  
1620  
1621  
1622  
1623  
1624  
1625  
1626  
1627  
1628  
1629  
1630  
1631  
1632  
1633  
1634  
1635  
1636  
1637  
1638  
1639  
1640  
1641  
1642  
1643  
1644  
1645  
1646  
1647  
1648  
1649  
1650  
1651  
1652  
1653  
1654  
1655  
1656  
1657  
1658  
1659  
1660  
1661  
1662  
1663  
1664  
1665  
1666  
1667  
1668  
1669  
1670  
1671  
1672  
1673  
1674  
1675  
1676  
1677  
1678  
1679  
1680  
1681  
1682  
1683  
1684  
1685  
1686  
1687  
1688  
1689  
1690  
1691  
1692  
1693  
1694  
1695  
1696  
1697  
1698  
1699  
1700  
1701  
1702  
1703  
1704  
1705  
1706  
1707  
1708  
1709  
1710  
1711  
1712  
1713  
1714  
1715  
1716  
1717  
1718  
1719  
1720  
1721  
1722  
1723  
1724  
1725  
1726  
1727  
1728  
1729  
1730  
1731  
1732  
1733  
1734  
1735  
1736  
1737  
1738  
1739  
1740  
1741  
1742  
1743  
1744  
1745  
1746  
1747  
1748  
1749  
1750  
1751  
1752  
1753  
1754  
1755  
1756  
1757  
1758  
1759  
1760  
1761  
1762  
1763  
1764  
1765  
1766  
1767  
1768  
1769  
1770  
1771  
1772  
1773  
1774  
1775  
1776  
1777  
1778  
1779  
1780  
1781  
1782  
1783  
1784  
1785  
1786  
1787  
1788  
1789  
1790  
1791  
1792  
1793  
1794  
1795  
1796  
1797  
1798  
1799  
1800  
1801  
1802  
1803  
1804  
1805  
1806  
1807  
1808  
1809  
1810  
1811  
1812  
1813  
1814  
1815  
1816  
1817  
1818  
1819  
1820  
1821  
1822  
1823  
1824  
1825  
1826  
1827  
1828  
1829  
1830  
1831  
1832  
1833  
1834  
1835  
1836  
1837  
1838  
1839  
1840  
1841  
1842  
1843  
1844  
1845  
1846  
1847  
1848  
1849  
1850  
1851  
1852  
1853  
1854  
1855  
1856  
1857  
1858  
1859  
1860  
1861  
1862  
1863  
1864  
1865  
1866  
1867  
1868  
1869  
1870  
1871  
1872  
1873  
1874  
1875  
1876  
1877  
1878  
1879  
1880  
1881  
1882  
1883  
1884  
1885  
1886  
1887  
1888  
1889  
1890  
1891  
1892  
1893  
1894  
1895  
1896  
1897  
1898  
1899  
1900  
1901  
1902  
1903  
1904  
1905  
1906  
1907  
1908  
1909  
1910  
1911  
1912  
1913  
1914  
1915  
1916  
1917  
1918  
1919  
1920  
1921  
1922  
1923  
1924  
1925  
1926  
1927  
1928  
1929  
1930  
1931  
1932  
1933  
1934  
1935  
1936  
1937  
1938  
1939  
1940  
1941  
1942  
1943  
1944  
1945  
1946  
1947  
1948  
1949  
1950  
1951  
1952  
1953  
1954  
1955  
1956  
1957  
1958  
1959  
1960  
1961  
1962  
1963  
1964  
1965  
1966  
1967  
1968  
1969  
1970  
1971  
1972  
1973  
1974  
1975  
1976  
1977  
1978  
1979  
1980  
1981  
1982  
1983  
1984  
1985  
1986  
1987  
1988  
1989  
1990  
1991  
1992  
1993  
1994  
1995  
1996  
1997  
1998  
1999  
2000  
2001  
2002  
2003  
2004  
2005  
2006  
2007  
2008  
2009  
2010  
2011  
2012  
2013  
2014  
2015  
2016  
2017  
2018  
2019  
2020  
2021  
2022  
2023  
2024  
2025  
2026  
2027  
2028  
2029  
2030  
2031  
2032  
2033  
2034  
2035  
2036  
2037  
2038  
2039  
2040  
2041  
2042  
2043  
2044  
2045  
2046  
2047  
2048  
2049  
2050  
2051  
2052  
2053  
2054  
2055  
2056  
2057  
2058  
2059  
2060  
2061  
2062  
2063  
2064  
2065  
2066  
2067  
2068  
2069  
2070  
2071  
2072  
2073  
2074  
2075  
2076  
2077  
2078  
2079  
2080  
2081  
2082  
2083  
2084  
2085  
2086  
2087  
2088  
2089  
2090  
2091  
2092  
2093  
2094  
2095  
2096  
2097  
2098  
2099  
2100  
2101  
2102  
2103  
2104  
2105  
2106  
2107  
2108  
2109  
2110  
2111  
2112  
2113  
2114  
2115  
2116  
2117  
2118  
2119  
2120  
2121  
2122  
2123  
2124  
2125  
2126  
2127  
2128  
2129  
2130  
2131  
2132  
2133  
2134  
2135  
2136  
2137  
2138  
2139  
2140  
2141  
2142  
2143  
2144  
2145  
2146  
2147  
2148  
2149  
2150  
2151  
2152  
2153  
2154  
2155  
2156  
2157  
2158  
2159  
2160  
2161  
2162  
2163  
2164  
2165  
2166  
2167  
2

### Abstract

We investigate the linear stability of static coronal-loop models undergoing thermal perturbations. The effect of conditions at the loop base on the stability properties of the models is considered in detail. We consider the question of appropriate boundary conditions at the loop base and conclude that the most physical assumptions are that the temperature and density (or pressure) perturbations vanish there. However, if the base is taken to be sufficiently deep in the chromosphere, either several chromospheric scale heights or several coronal loop lengths in depth, then the effect of the boundary conditions on loop stability becomes negligible so that all physically acceptable conditions are equally appropriate. For example, one could as well assume that the velocity vanishes at the base.

We calculate the growth rates and eigenmodes of static models in which gravity is neglected and in which the coronal heating is a relatively simple function, either constant per-unit mass or per-unit volume. We find that all such models are unstable with a growth rate of the order of the coronal cooling time. The physical implications of these results for the solar corona and transition region are discussed.



Accession For	
NTIS GRA&I	<input checked="checked" type="checkbox"/>
DTIC TAB	<input type="checkbox"/>
Unannounced	<input type="checkbox"/>
Justification	
By	
Date	
Dist	
AH	

## I. Introduction

For some time now static models of coronal loops (e.g., Rosner, Tucker, and Vaiana 1978; Craig, McClymont, and Underwood 1978; Vesecky, Antiochos, and Underwood 1979) have been widely used to interpret observations of both solar and stellar coronae (e.g., Bonnett and Dupree 1980, Orrall 1981). The key assumption in these models is that the energy input to the corona is constant in time so that a static solution to the relevant equations is possible. However, even if a static solution is mathematically possible, it will not be physically realizable unless this solution is also stable to small amplitude perturbations. It is well known that the coronal plasma is susceptible to a thermal instability due to the form of the dependence of radiative loss rate on temperature (Field 1965). Therefore, in order to assess their degree of validity, it is necessary to determine whether the static models are thermally stable or unstable.

The linear theory for the thermal stability of static coronal-loop models has been investigated by a number of authors, but with differing conclusions. In his original work, Antiochos (1979) concluded that the static models were thermally unstable. Similar results were obtained by Hood and Priest (1980). However, Chiuderi, Einaudi, and Torricelli-Ciamponi (1981); Craig and McClymont (1981); and McClymont and Craig (1981a,b,c) have found that the models are either stable or that the growth rates for instability are too small to be physically significant. The origin of this difference in the results of the two sets of authors is in their treatment of the base of the loop models. Antiochos (1979) and Hood and Priest (1980) have not included cool material,  $T < 10^5$  K, in their model, for which the form of radiative loss curve (e.g., Raymond, Cox, and Smith 1976) favors linear stability (Field 1965). In addition, Antiochos

has considered only perturbations with a vanishing first-order heat flux at the base. Chiuderi, Einaudi and Torricelli-Ciamponi; and Craig and McClymont argue that the growth rates for instability are very sensitive to these assumptions so that the models can be effectively stabilized either by including chromospheric material in the model (Craig and McClymont 1981) or by changing the boundary conditions so that the temperature perturbation, instead of the heat-flux perturbation, is assumed to vanish at the base (Chiuderi, Einaudi, and Torricelli-Ciamponi 1981).

The reason for this apparently high sensitivity of the models to the base conditions lies in one of the well-known properties of the static models: the fact that the magnitude of the conduction and radiation terms in the energy balance are approximately equal throughout the loop (Vesecky, Antiochos, and Underwood 1978). As discussed by Field (1965), we expect thermal instability in coronal plasma whose structure is such that radiation dominates. On the other hand, we expect stability if the structure is conduction dominated, since conduction always acts to damp out any temperature perturbation. Hence, the static models, whose structure is such that these two terms are comparable, are perched near the boundary separating stability from instability. Even seemingly minor changes on the form of the base or of the boundary conditions at the base can be sufficient to push the models to one side or the other of this boundary.

It is clear, therefore, that the proper treatment of the base is critical for determining to what extent the models are either stable or unstable. In the next section we discuss the question of the base conditions in detail. In Sections III and IV we calculate growth rates and eigenmodes for various static models and for various boundary conditions. In the final section, V, we discuss the implications of our results.

## II. Boundary Conditions

As an aid to determining the appropriate boundary conditions, let us first write down the perturbation equations for a one-dimensional loop model. Assuming that all physical variables are of the form:

$$f(s,t) = f_0(s) + e^{\nu t} f_1(s) \quad , \quad (1)$$

and assuming that the growth or damping time  $1/\nu$  is slow compared to the sound travel time so that the acceleration terms can be neglected in the momentum equation, we obtain (Field 1965, Antiochos 1979):

$$\nu n_1 + \frac{1}{A} \frac{d}{ds} (A n_0 v_1) = 0 \quad (2)$$

$$\frac{d}{ds} P_1 = m n_1 g_{||} \quad (3)$$

$$3/2 (\nu p_1 + v_1 \frac{d}{ds} P_0) - 5/2 \frac{P_0}{n_0} (\nu n_1 + v_1 \frac{d}{ds} n_0) + \frac{1}{A} \frac{d}{ds} (A F_1) = \mathcal{L}_1 \quad (4)$$

and

$$\frac{P_1}{P_0} = \frac{n_1}{n_0} + \frac{T_1}{T_0} \quad , \quad (5)$$

where:  $A(s)$  is the cross-sectional area of the loop;  $g_{||}(s)$  is the component of gravity parallel to the loop;  $F_1$  is the perturbed heat flux, which for the Spitzer (1962) conductivity is given explicitly by:

$$F_1 = - 10^{-6} \frac{d}{ds} (T_0^{5/2} T_1) \quad . \quad (6)$$

$\mathcal{L}_1$  constitutes the perturbed energy sources and sinks of the plasma. For optically thin radiative losses and for a coronal heating function that depends only on density and temperature or, equivalently, pressure and temperature,  $\mathcal{L}_1$  is given explicitly by (Antiochos 1979):



$$\mathcal{L}_1 = -2n_0 n_1 \Lambda(T_0) - n_0^2 \frac{d\Lambda}{dT_0} T_1 + \frac{\partial \epsilon}{\partial P_0} P_1 + \frac{\partial \epsilon}{\partial T_0} T_1, \quad (7)$$

where  $\Lambda(T)$  is the radiative loss coefficient (e.g., Cox and Tucker 1969) and  $\epsilon(p, T)$  is the coronal heating rate. The equilibrium profiles are, of course, given by (e.g., Vesecky, Antiochos, and Underwood 1979):

$$\frac{d}{ds} P_0 = m n_0 g_{||} \quad (8a)$$

$$-\frac{10^{-6}}{A} \frac{d}{ds} \left( A T_0^{5/2} \frac{dT_0}{ds} \right) = \mathcal{L}_0 = -n_0^2 \Lambda(T_0) + \epsilon(P_0, T_0) \quad (8b)$$

Note that we have neglected in equations (2) - (8) effects due to changes in ionization equilibrium or to optically thick radiation, both of which are clearly important in the chromosphere. Hence, this model cannot be used to determine the stability of the true solar chromosphere. We use this model chromosphere only for investigating the effect of having thermally stable material at the base of the corona and transition region. Since our results will turn out to be insensitive to the detailed structure of this region, we expect that our analysis will also be applicable to the solar chromosphere as long as it is thermally stable as well.

It is evident from the equations above that there are four independent spatial derivatives in the problem, which implies that four boundary conditions are required. This is to be expected since the full nonlinear equations also require four spatial boundary conditions for a unique solution (e.g., Richtmyer and Morton 1967). The usual situation is that at end of the loop two boundary conditions are specified. One condition generally relates to the thermal properties of the base; for example, with respect to the perturbation the loop base may act as a thermal bath, in which case the appropriate condition is that the temperature perturbation vanishes there,  $T_{1b} = 0$ ; or it may act as a thermal insulator so that the

perturbation heat flux vanishes there,  $F_{1b} = 0$ . The other condition generally relates to the inertial properties of the base; for example, it may act as a rigid wall with respect to the perturbation so that the velocity vanishes,  $V_{1b} = 0$ , or a "free surface," so that the pressure perturbation,  $P_{1b} = 0$ . Most of the discussion in the literature has concerned these four conditions, and the discussion in this paper will also concentrate on these four. Let us emphasize, however, that there are an infinite number of other possible boundary conditions and that, lacking some physical justification, there is no reason to single out the four above. A priori, all conditions are equally acceptable.

There has also been a considerable discussion in the literature on the distinction between symmetric and antisymmetric modes. However, this distinction is spurious. It is due only to the special class of models considered by the previous authors (Antiochos 1979; Hood and Priest 1980; Chiuderi, Einaudi, and Torricelli-Ciamponi 1981; Craig and McClymont 1981). In their models gravity is neglected, and the loop area and the coronal heating do not have any spatial variation. Under these simplifications, the static equations are autonomous, and the equilibrium models are symmetric about the loop apex. Hence, the solutions to the first-order equations, i.e., the normal modes of the loop, are either purely symmetric or antisymmetric about the apex. These results will clearly not hold for a realistic equilibrium model that has no special symmetry properties. For such a model each choice of four boundary conditions will, in general, determine a complete and distinct set of eigenvalues and eigenfunctions. Within each set all the modes are equally valid. Hence, in this paper we will avoid any discussion in terms of symmetric or antisymmetric modes; and since the most important mode from the viewpoint of thermal instability is the lowest order one, we will concentrate on the fundamental.

The question remains as to what choice of boundary conditions best represents the physical situation at the base of a solar loop. Ideally, one would like conditions at the loop base not to affect the stability properties of the corona and transition region. The standard procedure for achieving this is to place the base sufficiently far that over the time scale of any instability no effects can propagate to the base. However, the sound travel time in the corona, chromosphere and even photosphere is very rapid compared to typical thermal time scales, such as the coronal cooling time. On this time scale, material at the loop base is always in contact with the coronal plasma, even if the base is assumed to be in the photosphere. Note that our neglect of the acceleration terms in the force equation is tantamount to assuming an infinite sound speed and, consequently, a negligible propagation time scale throughout the loop. For such a model it is not obvious, at least to us, whether the position of the base can ever be chosen so that conditions there have an insignificant effect on the behavior of the corona. We show below that, fortunately, even with the rapid sound speed, the base has a negligible influence on the coronal stability if it is placed sufficiently deep.

In order to determine the physically valid boundary conditions to impose at the loop base, we need a definite model for this base region. As a simple model let us assume that the chromosphere below a coronal loop is isothermal at temperature  $T_b$ , is in hydrostatic equilibrium, and is strictly stable. In addition, we assume there is no real end point to a solar loop, so this model base region extends below the corona and transition region to arbitrarily large depths, i.e., either to many chromospheric scale heights or to depths large compared to the coronal loop length. Finally, let us neglect the curvature of the loop for this analysis and set  $g_{||}(s)$  to be a constant.

The form of the boundary conditions follows simply from the requirement that, since we are interested in coronal disturbances, the perturbations should vanish or at least remain finite in the chromosphere. Combining equations (3) and (5), an expression can be obtained for the pressure perturbation  $P$  in terms of the temperature perturbation  $T_1$  :

$$\frac{P_1(s)}{P_0(s)} = \frac{P_1(0)}{P_0(0)} - \int_0^s \frac{T_1}{T_0} \frac{ds}{H(T_0)} \quad , \quad (9)$$

where  $H(T_0)$  is the gravitational scale height at temperature  $T_0$  :

$$H(T) \equiv \frac{2kT}{mg_{||}} \quad (10)$$

and  $s = 0$  is some reference point in the loop (the top is convenient). We are defining  $s$  to increase downwards. It is evident from (9) that in order for  $P_1(s)$  to remain finite with increasing depth in the chromosphere, i.e.,  $s \rightarrow \infty$ , the temperature perturbation must vanish with depth  $T_1 \rightarrow 0$ . In fact,  $T_1$  must decay quite rapidly with depth, on the size scale of the chromospheric scale height  $H(T_b)$  or less, because the equilibrium pressure  $P_0$  grows exponentially on this size scale. Note that we are excluding the possibility of modes that oscillate indefinitely with depth. We are interested primarily in the lowest order mode; and as we will see below, this usually has no zero crossings.

We conclude, therefore, that the proper thermal boundary condition is that  $T_{1b} = 0$ . This result is to be expected physically. It follows from the fact that any perturbation of the temperature also implies a perturbation of the gravitational scale height. If the temperature disturbance extends more than a scale height or so deep into the atmosphere, a very large pressure disturbance must result due to the change in scale height. Hence, the only physically acceptable temperature perturbations are those that vanish on the order of a scale height or less.

Now, to determine the inertial boundary condition, we integrate the continuity equation (2) to obtain an expression for the particle flux  $n_0 v_1$  in terms of the density perturbation  $n_1$ :

$$n_0(s)v_1(s) = n_0(0)v_1(0) - v \int_0^s n_1 ds \quad (11)$$

As in the situation above, it is evident that in order for  $n_0 v_1$  to remain finite as  $s \rightarrow \infty$ ,  $n_1$  must vanish with depth. Again, this is to be expected physically. If the density disturbance extends over a large depth, then the change in the total number of particles in this region must be large, and consequently a large flux of particles into or out of the region must result. It is evident from (11) that in the chromosphere  $n_1$  must vanish faster than  $L_c/s$ , where  $L_c$  is the size scale of the coronal portion of the loop, i.e., the region where we expect a finite  $n_1$ . Note that the density perturbation may extend to much greater depths than the temperature one. We found above that  $T_1$  must vanish at least as fast as  $\exp(-s/H_b)$ , where  $H_b$  is the gravitational scale height in the chromosphere. For typical solar loops  $H_b \ll L_c$ .

We conclude that the proper boundary conditions at the loop base are that  $T_{1b} = 0$  and  $n_{1b} = 0$ . At any finite depth this is equivalent to the set  $T_{1b} = 0$  and  $P_{1b} = 0$ . Although the temperature, density, and pressure perturbations vanish, the mass flux does not. Using (2) and (3), the perturbed mass flux can be related to the pressure perturbation:

$$n_0 v_1 = n_0(0)v_1(0) - \frac{v}{mg_{||}} (P_1(s) - P_1(0)) \quad (12)$$

Since the pressure perturbation vanishes with depth, the mass flux will in general tend to some finite constant, corresponding to a steady-state flow in the chromosphere and below. This is to be expected on physical grounds as well. We do not expect the temperature and density structure deep in

the chromosphere or photosphere to be affected by a disturbance in the corona. However, if as in our problem, the time scale of the disturbance is long compared to the sound travel time, then a steady flow must occur at large depths to support any coronal flows. Of course, the velocity itself,  $V_1$ , vanishes with depth since the density  $n_0$  increases; however, the mass flux  $n_0 V_1$  stays constant. This is exactly the situation that we found for the case of evaporative cooling of coronal loops (Antiochos and Sturrock 1978). There again, the coronal evolution occurred on time scales long compared to the sound travel time, and it was found that a steady flow was set up at the loop base due to evaporative motions in the corona. This is also the situation for the photosphere at the base of an open magnetic field region such as in a coronal hole. In these regions coronal heating results in a steady solar wind flow. The presence of this flow has no observable effect on photospheric temperatures and pressures, but it clearly implies the existence of a mass flux in the photosphere equal to the coronal mass flux.

Let us now examine the effect of using different boundary conditions at the loop base, in particular, the rigid-wall one. We wish to find out how the coronal perturbation depends on the base conditions, for example, how  $P_1(0)$  depends on  $n_{0b} V_{1b}$ . From (12) it is evident that specifying the base mass flux is equivalent to specifying the base pressure perturbation, but the relation between  $P_1(0)$  and  $P_{1b}$  is given by (9):

$$P_1(0) = \frac{P_0(0)}{P_{0b}} P_{1b} + P_0(0) \int_0^L \frac{T_1}{T_0} \frac{ds}{H(T_0)} \quad (13)$$

Equation (13) is the key result. The effect on the coronal perturbation  $P_1(0)$  of assuming a non-vanishing  $P_{1b}$  is given by the first term on the right-hand side of (13). This term is of order  $P_0(0)/P_{0b}$  for a temperature perturbation that vanishes rapidly in the chromosphere so that the pressure

$C = 10$  and  $m = 3$ . This value for  $m$  is convenient numerically since for  $m = 3$  the depth of the base region turns out to be proportional to  $1/\delta$ ; hence, the range of chromospheric depths covered by the range used for  $\delta$  is correspondingly large,  $(L - L_c)/L_c$  ranges from  $\sim 10^{-5}$  to  $\sim 10$ . Again, we note that there is almost no variation in  $\nu$  irrespective of the depth of the chromosphere.

We have investigated the effect of the form of the coronal heating on stability by performing a series of calculations as in Figure 3 for the case of uniform heating per unit volume,  $\gamma = 0$ . The results are essentially identical to those shown in Figure 3. This agrees with our previous calculations (Antiochos 1979) in which we investigated a wide range of values for  $\gamma$  and found no significant effect on the growth rate.

We have also looked for any possible effect due to the form of the chromospheric heating by varying the exponent  $m$  defined in (43). This parameter determines the degree of stability of the chromosphere, i.e., the magnitude of the quantity  $(T_0 \frac{\partial f}{\partial T_0})$  (cf., Field 1965). The chromospheric magnitude of this quantity is small in our models compared to its coronal value except for the case  $m = 1$ . Note that for  $m = 1$  the chromospheric depth  $L - L_c$  varies only as  $\ln(1/\delta)$  so that even with the smallest value of  $\delta$  usable numerically,  $\sim 10^{-15}$ , the chromospheric depth is not large,  $(L - L_c)/L_c \sim .05$ . The results for the cases with  $m = 1$  are identical to those shown in Figure 3 for the case  $m = 3$ . Again, there is no significant dependence of the growth rate  $\nu$  on either the base temperature or the chromospheric depth. We conclude that the instability does not depend on the particular form, (42), that we assumed for the chromospheric heating.

This result is to be expected. For temperatures  $\lesssim 5 \times 10^4$  K, the quantity  $T_0 \frac{\partial f}{\partial T_0}$  is strictly negative in all our models; hence, this region cannot contribute to any instability. As we will see below, the unstable

obtained by solving (14) for a series of static models with different base properties. These static models all have very similar coronal properties. The apex temperature  $T_0(0)$  was chosen in each case to be  $10^6$  K and the coronal heating given by  $\gamma = 1$  and  $Q = 10^{-12}$  ergs/sec/particle, equation (41). Given the coronal temperature and heating rate, then as is well known (e.g., Vesecky, Antiochos, and Underwood 1979), the coronal density and coronal loop length are constrained by the scaling laws. They turn out to be  $n_0(0) = 3.2 \times 10^9 \text{ cm}^{-3}$  and  $L_c = 5.2 \times 10^8 \text{ cm}$ . Conditions at the base, however, are very insensitive to the coronal conditions, so that we can vary the base temperature and the amount of base material with almost no change in coronal parameters.

In our model the base temperature is given by  $T_b$ , and the depth of the chromosphere is determined primarily by the constant  $\delta$ , equation (43). Hence, there are actually two distinct sets of models in Figure 3. In one set all the models have a value of  $\delta \approx 1$ , which implies that there is an insignificant amount of material at the base. These models correspond to the usual static-loop models, as in Vesecky, Antiochos, and Underwood (1979). For such models we investigated the effect of the base temperature on stability by varying  $T_b$  from  $2 \times 10^5$  K to  $10^4$  K. In Figure 3 only the cases down to  $T_b = 3 \times 10^4$  K are shown, but no change was observed in using  $T_b$  down to  $10^4$ . As is clear from the figure, the value of the base temperature has essentially no effect on loop stability. The growth rate  $\nu$  is of order unity irrespective of whether  $T_b$  is chosen to occur at chromospheric or transition-region temperatures.

The second set of models in Figure 3 are those with a fixed base temperature  $T_b = 3 \times 10^4$  K, but with varying amounts of base material at this temperature. The value of  $\delta$  was varied from  $\delta = 1$  to  $\delta = 5 \times 10^{-6}$ . The other parameters in the energy input rate (equation (42)) were fixed,



such as the VAL models (Vernazza, Avrett and Loesser 1981), all indicate the presence of a flat temperature "plateau" at  $T \sim 2 \times 10^4$  K with a very abrupt rise at higher temperatures. Within the context of the static model, and neglecting possible kinetic effects (Shoub 1983), the only way to obtain the observed very sharp structure in the temperature profile is to have a correspondingly sharp structure in the energy input rate. This is one reason why the static models are generally assumed to have a base above  $2 \times 10^4$  K. The particular form, (41) and (42) is chosen simply for convenience. It permits us to investigate the effects of adding a varying amount of cool, radiatively stable material to the loop base.

## b) Growth Rates

### (1) Free Surface

We have calculated the eigenvalues  $\lambda$  for a wide range of static models. In particular, we have determined the dependence of the stability on the following properties of the model: the coronal temperature, the base temperature, the depth of the chromosphere, the form for the heating and, of course, the boundary conditions. The main result of this analysis is that for the boundary conditions  $T_{1b} = 0$ ,  $n_{1b} = 0$ , all the models were unstable with a growth time approximately equal to the coronal cooling time. The growth rate was found to be completely insensitive to the loop temperature either in the corona or base, to the amount of chromospheric material or to the form of the chromospheric heating. Hence, we conclude that the instability is a true physical one and will occur in solar loops that satisfy our basic assumptions, i.e., spatial variations in the loop area and heating, and the effects of gravity can be neglected.

Figure 3 shows the growth rate  $\gamma$  of the lowest free-surface mode

$T < 5 \times 10^4$  K. In order for the model to have a large chromosphere, the temperature gradients and, hence, the heat flux must be small at these temperatures. The radiation losses in the chromosphere cannot be balanced by conduction from above (e.g., Athay 1981); thus for a static model these losses must be balanced by the energy input (e.g., Craig, Robb and Rollo 1982).

Therefore, we use the following form for the energy input:

$$\epsilon = Qn^\gamma \tanh(\chi(T)) + n^2 \Lambda (1 - \tanh(\chi(T))) , \quad (41)$$

where

$$\chi(T) = C (T/T_b - 1 + \delta)^m \quad (42)$$

and  $Q, \gamma, C, m$  and  $\delta$  are constants. Equations (41) and (42) imply that for  $\delta \ll 1$ :

$$\epsilon \rightarrow \begin{cases} Qn^\gamma , & \text{for } T > T_b \\ n^2 \Lambda , & \text{for } T = T_b \end{cases} , \quad (43)$$

i.e., the energy input rate tends to  $Qn^\gamma$  for temperatures larger than the base temperatures and tends to the radiative loss rate at the base temperature. The values 0 and 1 for  $\gamma$  correspond to constant coronal heating per unit volume and per unit mass, respectively. The depth of material at the base temperature is determined by the value of  $\delta$ ; it becomes arbitrarily large for arbitrarily small  $\delta$ .

The form that we assume for the energy input, (41) and (42) may appear highly unphysical because it undergoes an abrupt although continuous change near  $T = T_b$ . However, such a sharp structure in the energy input rate is implied by the observations. Empirical models of the upper chromosphere,

chromosphere. This makes it impossible to use a uniform grid for finite differencing the independent variable  $x$ . However, we cannot use the equilibrium temperature  $T_0$  as the independent variable since the temperature gradient vanishes at the loop apex and base. Instead, we define a new independent variable  $r$ :

$$dr = \left( \frac{T_0(0)}{T_0} \right)^2 \left( 1 - \left( 1 - \frac{T_b}{T_0(0)} \right) \frac{T_b}{T_0} \right)^2 dx \quad (40)$$

and use a uniform grid in  $r$ . It is evident from (30) that the effect of transforming to  $r$  is to increase the number of grid points at transition region temperatures ( $T_0(0) < T_0 < T_b$ ) by a factor of order  $(T_0(0)/T_0)^2$ . We found that this was sufficient to yield an accurate solution.

#### a) Form of Heating and Cooling

There are two functions in the problem that have yet to be specified: the radiative loss coefficient,  $\Lambda(T)$ , and the energy input rate  $\epsilon(n, T)$ . For the former we use a smooth analytic approximation to the curve derived by Raymond, Cox and Smith (1976). Figure 2 shows this curve along with our approximation to it. The stability properties of the models are not sensitive to the exact form of  $\Lambda(T)$  as long as this form is such that it implies radiative instability above  $\sim 10^5$  K and stability below.

Since the mechanism for coronal heating is not known, the form of the energy input  $\epsilon$  is essentially arbitrary. In our previous work we found that the stability properties are insensitive to the exact form for  $\epsilon$ , at least, for the case where this form is a power-law dependence on  $n$  and  $T$ . Hence, we simply assume that in the corona and transition region the energy input either per unit volume or per particle is constant. At lower temperatures a different form for the energy input must be used in order to have a significant mass of material at "chromospheric" temperature,

models the growth time  $1/\nu_f$  is very short, of order the cooling time in the transition region rather than that in the corona (Antiochos 1979). We find that for these cases the rigid-wall growth rate  $\nu_r$  is slightly larger than  $\nu_f$ . However, for models in which some cool stable material occurs at the base, the rigid-wall boundary conditions always result in smaller growth rates.

#### IV. Numerical Results

The mathematical problem that must be solved is now clearly defined. For the free-surface conditions, (14) reduces to a standard Sturm-Liouville problem, as in Antiochos (1979), which we solve in exactly the same manner as before.

For the rigid-wall conditions, the inhomogeneous problem must be solved subject to the constraint (24a). Note that this is not a standard Sturm-Liouville problem; hence, none of the well-known theorems (e.g., Morse and Feshbach 1953) on the behavior of the eigenfunctions and eigenvalues need apply. There are two parameters,  $\lambda$  and  $\eta$ , that must be determined; therefore, we do not use a "shooting" technique as in the homogeneous case to obtain solutions. First, we note that since  $\eta$  will, in general, be non-zero for any finite-length loop, we can eliminate it by defining a new dependent variable ( $\mu/\eta$ ). Now (14) and (24a) define a nonlinear boundary-value problem for ( $\mu/\eta$ ) and the unknown parameter  $\lambda$ . This is solved by standard techniques: Newton-Raphson iteration and finite-difference solution of the linearized equations. Convergence was rapid,  $\leq 20$  iterations for all the cases we investigated.

One numerical complication is the extreme variation in temperature scale height between the corona, the transition region, and the

order mode, has no zero crossings and its normalization is irrelevant, the sign of  $\delta v$  is determined primarily by the sign of the terms in the brackets in the rightmost integral; however, this factor does not have a unique sign. The first term  $v_f$  is always positive and for models of interest has magnitude  $\sim 1/\tau$ ; consequently, it enhances instability. The sum of the second and third term is proportional to  $(-\epsilon/P_0)$  for the case where the heating  $\epsilon$  is constant per particle, and  $(-2\epsilon/P_0)$  for  $\epsilon$  constant per unit volume. Hence, the contribution from the last two terms is negative, and since in the static model the energy input and the radiative losses are roughly equal in the corona (e.g., Vesecky, Antiochos, and Underwood 1979),  $\epsilon/P_0$  is also of order  $1/\tau$ . It is, therefore, not clear which of the two contributions will dominate; however, it turns out that the negative contribution is usually larger than the positive one so that the rigid wall has a net stabilizing effect.

This is to be expected physically. A rigid wall acts to inhibit flows and, consequently, any density disturbance. For optically thin radiation at coronal temperatures, both the temperature dependence and the density dependence of the losses is such as to promote instability (Field 1965). By suppressing the density effect, a rigid wall tends to weaken the instability. It is interesting to note that this need not always be the case. Sometimes a rigid wall can actually enhance instability. In particular, if  $v_f$  is very large and dominates the other terms in (39), we would expect  $\delta v$  to be positive. This situation does occur for models in which the base is placed high up in the transition region and the temperature boundary condition is assumed to be  $dT_{1b}/ds = 0$ . For such

the particular solution:

$$\zeta_r \rightarrow \frac{2}{5} \eta_r y_b^{5/14} \frac{(v_r \tau_b - 5/2)}{(v_r \tau_b + 1)} \quad (35)$$

If, as expected,  $v_r \sim 0(1/\tau)$ , then for  $\tau/\tau_b \rightarrow 0$

$$\zeta_r \rightarrow \frac{2}{5} \eta_r y_b^{5/14} \quad (36)$$

We will see below that (35) also agrees with exact solution of (14).

These results verify our claim that  $\eta_r$  decays as  $L_c/L$ . We have that

$$\eta_r = \int_0^{L_c/L} \zeta_r y^{-5/14} dx + \int_{L_c/L}^1 \zeta_r y^{-5/14} dx \quad (37)$$

Substituting the asymptotic form (35), or (36), into the second integral yields (26) to within a factor of order unity.

The effect on the growth rate of imposing a rigid-wall constraint can also be estimated. Using the equations for  $\zeta_f$  and  $\zeta_r$ , and their boundary conditions, the following expression is obtained:

$$\delta\lambda = \lambda_r - \lambda_f = \frac{\lambda_f \int_0^1 \zeta_f f(x) dx + \int_0^1 \zeta_f g(x) dx}{\int_0^1 \frac{\zeta_f \zeta_r}{\eta_r} dx - \int_0^1 \zeta_f f(x) dx} \quad (38)$$

If  $L_c/L \ll 1$ , then to lowest order in  $L_c/L$ , Equation (38) can be written as:

$$\delta v = v_r - v_f = \left( \frac{\int_0^1 \zeta_f y^{-5/14} dx}{\int_0^1 \zeta_f^2 dx} \right) \int_0^1 y^{5/14} \zeta_f \frac{2}{5} \left( v_f - \frac{2f}{P_0} + \frac{\partial f}{\partial P_0} \right) dx \quad (39)$$

Each of the integrals in (39) is of order  $L_c/L$ ; hence,  $\delta v$  is also of this order.

Depending on the sign of  $\delta v$ , the rigid-wall can have a stabilizing ( $\delta v$  negative) or destabilizing ( $\delta v$  positive) influence. Since  $\zeta_f$ , the lowest

The longest length scale for the decay is obtained in the limit  $\tau/\tau_b \rightarrow 0$ . This length,  $\sim L_c (T_b/T_0(0))^{7/4}$ , is typically small compared to physical size scales either in the corona or chromosphere. We show below that the form predicted above is obtained from exact solution of (14).

We now consider the rigid-wall case. With  $\zeta_r$  as the dependent variable, Equation (14) becomes:

$$\frac{d}{dx} \left( y \frac{d}{dx} \zeta_r \right) + Q(x) \zeta_r + \lambda_r \zeta_r = \eta_r (\lambda_r f(x) + g(x)) , \quad (30)$$

where the subscript "r" is used to indicate rigid-wall quantities. The functions  $f$  and  $g$  are given by:

$$f(x) = \frac{2}{5} y^{5/14} \quad (31)$$

and

$$g(x) = -y^{5/14} \left( \frac{4}{7} \frac{d^2 y}{dx^2} + \alpha_{P_0} \frac{\partial \mathcal{F}}{\partial P_0} \right) . \quad (32)$$

Following the arguments above, in the base region, Equation (30) reduces to:

$$\begin{aligned} y_b \frac{d^2}{dx^2} \zeta_r - \left( \frac{L}{L_c} \right)^2 \frac{1}{\tau_b} \zeta_r - \left( \frac{L}{L_c} \right)^2 \tau \nu_r \zeta_r \\ \approx \eta_r y_b^{5/14} \left( \frac{L}{L_c} \right)^2 \left( -\frac{2}{5} \nu_r \tau + \tau/\tau_b \right) , \end{aligned} \quad (33)$$

where, again, due to the form of the radiative losses, we assume that:

$$\left( \frac{\partial \mathcal{F}}{\partial P_0} \right)_b \sim -1/\tau_b . \quad (34)$$

The general solution to (33) consists of a linear combination of the homogeneous and particular solutions. However, the homogeneous solution is equivalent to the free-surface solution, and we found above that this decays exponentially. Hence, the solution at large depths is dominated by

where the brackets indicate the average coronal value. Hence, for large depths,  $\eta$  decays as  $L_c/L$ . This is the same behavior that we found before, except that now since there is no gravity, the only scale in the problem is the coronal loop length, so that this length rather than the gravitational scale height determines the decay scale for the effects of the wall.

#### b) Asymptotic Forms

In order to check whether  $\zeta$  will, in fact, decrease rapidly in the chromosphere, let us examine the asymptotic forms for  $\zeta$  in this region as predicted by equation (14). We first consider the free-surface case. Since  $T_0$  is approximately constant in the chromosphere, Equation (14) reduces to:

$$y_b \frac{d^2}{dx^2} \zeta_f + \alpha \left( T_0 \frac{\partial f}{\partial T_0} \right)_b \zeta_f - \left( \frac{L}{L_c} \right)^2 v_f \tau \zeta_f = 0, \quad (27)$$

where the subscript "f" is used to refer to the free-surface variables. Assuming that the radiative loss function has a simple power-law dependence on  $T$ , and that the power is positive so that the chromosphere is radiatively stable, then we expect that:

$$\left( \frac{T_0}{P_0} \frac{\partial f}{\partial T_0} \right)_b \sim - \frac{f}{P_0} \sim - 1/\tau_b, \quad (28)$$

where  $\tau_b$  is the radiative cooling time at the base. Note that our definition for  $f$  has a sign change from that used by Field (1965) and that the negative sign is required for stability. Assuming that the free-surface growth rate,  $v_f$ , is of order the coronal cooling rate  $1/\tau$ , Equations (27) and (28) yield the following asymptotic form for  $\zeta$ ,

$$\zeta \sim e^{-s/\ell}$$

$$\text{where } \ell \approx L_c \left( \frac{T_b}{T_0(0)} \right)^{7/4} (1 + \tau/\tau_b)^{-1/2}. \quad (29)$$



The boundary conditions must now be specified. Assuming the "natural" ones,  $n_{1b} = T_{1b} = 0$  leads to:

$$\eta = 0 \quad \text{and} \quad \mu_b = 0 \quad (23)$$

at each end of the loop. Note that we have used the fact that the equilibrium heat flux vanishes at the base in order to derive Equation (23). If one assumes instead the rigid-wall conditions  $V_{1b} = T_{1b} = 0$ , this leads to the constraint (Antiochos 1979):

$$\int_0^1 \mu y^{-5/14} dx = 0 \quad (24a)$$

and the conditions:

$$\mu_b + y_b^{5/14} \eta = 0 \quad (24b)$$

With this formulation it is difficult to compare the effects of the two sets of boundary conditions since one set leads to homogeneous conditions on  $\mu$ , (23), whereas the other does not. In order to facilitate the comparison, let us for the moment reformulate the problem in terms of a new variable defined as  $\zeta = \mu + y^{5/14} \eta$ , so that the boundary conditions (24b) will become homogeneous. Hence, the problem reduces to solving an equation for  $\zeta$  and  $\eta$  of the form (14) (only the form of  $G(x)$  changes) and with boundary conditions:

$$\begin{aligned} \text{for free surface, } \zeta_b &= 0, \text{ and } \eta = 0; \\ \text{for rigid wall, } \zeta_b &= 0, \text{ and } \eta = \int_0^1 \zeta y^{-5/14} dx. \end{aligned} \quad (25)$$

The relation between the two sets of conditions is now transparent. We note that if, as expected,  $\zeta$  decreases sufficiently rapidly in the chromosphere, then (24) implies that in the limit of large chromospheric depths, i.e.,  $L_c/L \rightarrow 0$ ,

$$\eta \rightarrow (L_c/L) \langle \zeta y^{-5/14} \rangle, \quad (26)$$

Under the special assumptions above, the perturbation equations (2) - (6) can be simplified to a form essentially equivalent to the one we used previously (Antiochos 1979):

$$\frac{d}{dx} \left( y \frac{d}{dx} \mu \right) + Q(x) \mu + \lambda \mu = \eta G(x) , \quad (14)$$

where we have defined dimensionless variables:

$$x = s/L , \quad (15)$$

$L$  is the loop half-length,

$$y(x) \equiv (T_0/T_0(0))^{7/2} , \quad (16)$$

$$\mu \equiv \frac{y^{5/14}}{v} \frac{d}{ds} v_1 , \quad (17)$$

$$\text{and } \eta = \frac{P_1}{P_0} = \text{constant}. \quad (18)$$

The eigenvalue  $\lambda$  is defined as:

$$\lambda = - (L/L_c)^2 v \tau , \quad (19)$$

where  $\tau$  is given by the coronal cooling time scale

$$\tau = \frac{5}{2} \cdot 10^6 P_0 L_c^2 (T_0(0))^{-7/2} . \quad (20)$$

The functions  $Q(x)$  and  $G(x)$  are given by:

$$Q(x) = \frac{1}{14} \frac{d^2 y}{dx^2} - \frac{1}{y} \left( \frac{5}{14} \frac{dy}{dx} \right)^2 + \alpha \left( T_0 \frac{\partial f}{\partial T_0} \right) \quad (21a)$$

$$G(x) = -y^{5/14} \left( 3/5 \lambda + \frac{d^2 y}{dx^2} + \alpha T_0 \frac{\partial f}{\partial T_0} + \alpha P_0 \frac{\partial f}{\partial P_0} \right) . \quad (21b)$$

where  $\alpha$  is a constant of the dimensions:

$$\alpha = 10^6 L^2 (T_0(0))^{-7/2} \quad (22)$$

wall where the pressure  $P_{lb}$  jumps back up to its coronal value. The physical reason for this is straightforward. Flows in the corona will cause material either to pile up or to evacuate from the wall. Hence, there must exist a pressure gradient near the wall of the same order as the coronal gradient in order to decelerate or accelerate the flows. However, over most of the chromosphere the flows are in a steady state, and the pressure perturbation is negligible.

It is clear from these results that the appropriate boundary condition to assume at the loop base is that  $P_{lb} = 0$ . This condition results naturally in the chromosphere, irrespective of what is assumed at the base as long as the base is placed sufficiently deep. If the base is placed within several scale heights of the top of the chromosphere, then it is the only boundary condition that is appropriate; the use of rigid-wall conditions, or any others, is likely to lead to incorrect conclusions. If the base is placed many scale heights deep, then the particular boundary condition used becomes irrelevant.

### III. Analytic Results

#### a) Perturbation Equations

In this paper we calculate growth rates and eigenfunctions only for the simplified problem discussed by previous authors; we neglect gravity and any spatial variation in the loop area or heating function. We discuss the effects of gravity and the area variation in a subsequent paper (Antiochos and An 1985). For purposes of comparison, we calculate the growth rates and modes for several sets of boundary conditions, although as we discussed above, the physically appropriate ones are  $T_{lb} = 0$  and  $n_{lb} = 0$ .

perturbation there is of order the coronal one (i.e.,  $P_1(s)$  does not diverge exponentially in the chromosphere). For a base that is several scale heights deep,  $P_0(0)/P_{0b}$  is negligible; therefore, the form of the coronal perturbation is insensitive to the boundary condition on  $P_{1b}$  or, equivalently,  $V_{1b}$ .

The situation is clarified by Figure 1, where for a given  $T_1(s)$  we plot the resulting form of  $P_1(s)$  and  $n_0 V_1(s)$  for both rigid-wall  $V_{1b} = 0$  and free-surface  $P_{1b} = 0$  boundary conditions. Since this is for illustrative purposes only, we have taken an extremely simple equilibrium loop model in which we neglect the effects of gravity in the corona and assume that the transition region is vanishingly thin. The corona is, therefore, isothermal and isobaric and is defined to extend from  $s = 0$  to  $s = L_c$ . Below this corona is an isothermal chromosphere in hydrostatic equilibrium and with a temperature 100 times lower. The base of the loop model is taken to occur 10 chromospheric scale heights deep,  $L = L_c + 10 H_b$ . For simplicity, the temperature perturbation,  $T_1/T_0$ , is assumed to be constant in the corona and to decay exponentially in the chromosphere on a size scale of  $H_b/10$ .

The forms for  $P_1(s)$  and  $n_0 V_1(s)$  obtained from (9) and (11) are plotted in Figure 1a and 1b, respectively. We have taken the velocity to vanish at the top,  $V_1(0) = 0$ , which would be the case for the lowest order mode of a symmetric loop model. On the scale of this figure, the modes with  $P_{1b} = 0$  and those with  $V_{1b} = 0$  are indistinguishable except within a few scale heights of the base. In this boundary region the rigid wall mass flux exhibits a sudden decrease to zero, and  $P_1$  exhibits a sudden increase back up to its coronal value, i.e.,  $P_{1b} = P_1(0)$ . Note that the magnitude of this jump does not change with position of the base. No matter how deep the rigid wall is placed, there will occur a small boundary layer at the

modes have a vanishingly small amplitude in this region compared to coronal amplitudes.

#### (11) Rigid Wall

We have solved Equation (14) for the rigid-wall conditions (24) and for the exact wide range of equilibrium models used with the free-surface conditions. Some of the results are shown in Figure 3. The growth rate of the lowest rigid-wall mode is plotted for comparison with the corresponding free-surface mode. The rigid-wall rate is seen to approach the free-surface one as the chromospheric depth becomes large,  $L_c/L \ll 1$ ; the ratio of the growth rates is near unity,  $v_r/v_f = .85$  for the deepest model in the figure,  $L_c/L = .07$ . These numerical results confirm the analytic arguments above that for large depths the rigid-wall condition is equivalent to the free-surface one.

We find that the rigid-wall growth rates are also insensitive to the coronal temperature, the base temperature or the form of the heating. However, Figure 3 shows that they do depend on the depth of the base region. For models with  $L_c > L/2$ , the growth rate is negative, indicating stability. Note that this value for  $L_c/L$  actually implies a large chromospheric region. Since the base density is approximately two orders of magnitude greater than the coronal density, the bulk of the loop plasma is in the base for  $L_c/L = .5$ . Note also that the damping rate is almost constant for models with  $\delta \geq 10^{-2}$ . This result emphasizes the unphysical nature of the rigid-wall conditions and the danger in using them. If one assumes the rigid-wall condition and then considers models with increasing chromospheric depths, it first appears that static loops are stable and that the stability is insensitive to base conditions. One would naturally conclude that the models are physically stable. But as the base depth is

increased, the models suddenly become unstable. Somehow the addition of too much stable material at the base destabilizes the corona! This is clearly an unphysical result and is due to using improper assumptions at the onset.

The same type of behavior is found when boundary conditions other than  $T_{1b} = 0$  and  $n_{1b} = 0$  are used. For example, Craig and McClymont (1981) find that the conditions  $dT_{1b}/ds = 0$  and  $P_{1b} = 0$  lead to abrupt changes in the growth rate at very small chromospheric depths. We have also examined these conditions and a variety of others defined by the vanishing of a linear combination of  $T_{1b}$  and  $F_{1b}$  or  $P_{1b}$  and  $V_{1b}$ . Depending on the particular equilibrium model, the boundary conditions assumed can result in growth rates either larger or smaller than the free surface one; however, in all cases the rates tended to the free-surface result for large chromospheric depths. In all but the free-surface case the growth rates exhibited an abrupt change at some range of chromospheric depth; hence, the conditions  $T_{1b} = n_{1b} = 0$  are the only ones that are generally valid.

### c) Normal Modes

Along with the eigenvalues  $\lambda$  we have also calculated the eigenfunctions  $\mu$  for all the equilibrium models considered. Two representative cases are shown in Figures 4a and 4b. In Figure 4a we show both the free-surface  $T_1/T_0$  and the rigid-wall mode,  $T_1/\Lambda T_0$ , for the equilibrium model of Figure 3 with the deepest chromosphere ( $L_c/L = .07$  corresponding to  $\delta = 5 \times 10^{-6}$ ). In Figure 4b the results for the model with  $\delta = 10^{-3}$ , ( $L_c/L = .97$ ), are shown.

We first discuss the results for the deepest model, Fig. 4a. In order to resolve their structure in the transition region, the modes are plotted against a nonlinear distance scale. From the loop apex,  $s = 0$ , to a point

two coronal depths down,  $s = 2L_c$ , the equilibrium temperature  $T_0$  is used as the independent variable. From this depth down to the loop base,  $s = L$ , the distance itself is used. Of course, all the significant structure in the eigenmodes occurs well above the point  $s = 2L_c$ . The region below this depth is included in the figure only to point out that the numerical calculations verify the analytic asymptotic forms obtained above. Using (29) and taking  $\tau/\tau_b = 0$ , we find that the decay scale  $\ell$  for the free-surface mode is equal to  $2.16 \times 10^{-3} L_c$ . Hence, the free-surface mode should have essentially zero amplitude in the deep region. The numerical results agree with this. We find that the amplitude of  $T_1/T_0$  drops below computer accuracy well before  $s = 2L$ . On the other hand, the amplitude of the rigid-wall mode,  $T_1/\eta T_0$ , does not vanish. Instead, it has a constant value of 0.4 over most of the chromosphere and vanishes only near the base on the size scale  $\ell$ . This behavior is also in agreement with the analytic results. In the chromosphere,  $T_1/\eta T_0 = \zeta/\eta y^{5/14}$ ; therefore, from (36) we expect the mode to approach the value  $2/5$ , except very near the base, where it must vanish due to the boundary conditions.

It can be seen from Fig. 4a that the modes have significant amplitude only in the corona and transition region. The free-surface mode has been normalized to equal the rigid-wall value at the apex. Note that the rigid-wall quantity  $T_1/\eta T_0$  does not have an arbitrary normalization factor since this quantity is the ratio of the temperature-to-pressure perturbations. Its magnitude has physical significance. Our results indicate that the pressure perturbation is in the same sense but smaller than the temperature perturbation. As the depth of the chromospheric region increases,  $L_c/L \rightarrow 0$ , we find that the coronal magnitude of  $T_1/\eta T_0$  increases as  $(L_c/L)^{-1}$ . This confirms our previous result that  $\eta$  should decrease as  $L_c/L$  for a fixed temperature perturbation.

On the scale of Fig. 4a the two modes are almost identical in the corona and transition region. Only near the base is there a significant deviation; and as the depth of the base region is increased, the two modes become indistinguishable. The modes exhibit a strong peak near  $5 \times 10^4$  K. At approximately this temperature the radiative losses change from being a destabilizing to a stabilizing effect, so that below this temperature the modes decay very rapidly on the scale of  $\lambda$ . It is important to emphasize that although the modes peak strongly in the transition region, the instability is not a local one. The modes have finite amplitude throughout the corona, and the growth rates correspond to the coronal cooling time rather than the much faster cooling time in the transition region. Hence, the instability is a global one involving the complete loop except for the chromosphere.

The situation is somewhat different for the model with a shallower base, Fig. 4b. The free-surface mode is very similar to that of the model with the deeper base. Indeed, this mode is insensitive to just about everything; hence, the curve shown in Fig. 4a (or 4b) can be considered the universal form.

However, the rigid-wall mode is obviously very different from that of Fig. 4a. The most striking difference is that the mode has a zero crossing at the base of the transition region and is negative in the chromosphere. This is in agreement with the analytic results. We note from (35) that as  $\nu$  decreases from a large positive quantity, the asymptotic amplitude becomes negative. As  $\nu$  decreases further to a large negative quantity, the amplitude becomes positive again. The numerical results agree with the behavior. For models with large depths,  $\delta \ll 10^{-4}$ , the amplitude in the chromosphere is positive. For models with intermediate depths,  $\delta \sim 10^{-3}$ , it is negative. It becomes positive again for small depths,  $\delta > 10^{-2}$ . For



models without a very deep base, the chromospheric form of the rigid-wall mode is clearly quite sensitive to the exact position of the wall. The free-surface mode, on the other hand, shows no change for all values of  $\delta$  that we investigated.

In the corona the rigid-wall mode has the same general shape as that in Fig. 4a, but the amplitude is an order of magnitude smaller. This means that for a given amplitude temperature perturbation, the effect of the decrease in the base depth is an increase in the coronal pressure perturbation by an order of magnitude. In fact, the pressure perturbation actually has a larger coronal amplitude than the temperature perturbation. We note from Fig. 4b that the ratio of the temperature to pressure amplitude is less than unity for temperatures down to  $\sim 8 \times 10^5$  K. This region encompasses about 70 percent of the coronal portion of the loop. Since from (5)

$$\frac{T_1}{T_0 \eta} + \frac{n_1}{n_0 \eta} = 1 \quad , \quad (44)$$

our results imply that over most of the corona the temperature and density perturbations must be in the same sense. A decrease (an increase) in the temperature is accompanied by a decrease (an increase) in the density as well. Since a decrease in the temperature implies an increase in the radiative loss rate (for  $T > 10^5$  K), whereas a decrease in the density implies a decrease in the losses, the perturbations oppose each other as far as instability is concerned. The net result is stability,  $\nu < 0$  for the model in Fig. 4b. For models with a deeper base region, as in Fig. 4a, the temperature perturbation is much larger than the pressure perturbation, and, consequently, the density perturbation takes the opposite sense. Both the temperature and density disturbances act to promote instability, and the model of Fig. 4a is, indeed, unstable,  $\nu > 0$ . We conclude that the

stability of the rigid-wall models such as Fig. 4b is a boundary-condition effect. It is due solely to the assumption of a rigid-wall at a particular depth.

## V. Discussion

There are two key results of this paper. The first is that the appropriate boundary conditions to assume at the loop base are  $T_{1b} = n_{1b} = 0$ . For models with a sufficiently deep base ( $L_b \gg \min(H_b, L_c)$ ), all boundary conditions can be used; however, the set above is the only one that is appropriate for models that do not satisfy this condition. Indeed, we find it surprising just how universally valid these boundary conditions appear to be. Even for models with little or no chromosphere, they yield the correct growth rate and form of the eigenmode for the instability. Contrary to the conclusions of several authors (Habbal and Rosner 1979; Chiuderi, Einaudi, and Torricelli-Ciamponi 1981; Craig and McClymont 1981; and McClymont and Craig 1981a,b,c), the mere presence of radiatively stable material at the loop base does not stabilize the static models. If incorrect boundary conditions are used, then the base can act either to stabilize or, as we showed above, to destabilize the static models. However, if the proper conditions are used, then the amount of base material has no effect on the stability.

This is a convenient result from a numerical point of view. It is often quite difficult to handle numerical models with extremely deep base regions (e.g., Craig, Robb, and Rollo 1982). Our results indicate that models with very shallow bases can yield correct results if the correct boundary conditions are used.

The second main result of this paper is that under our assumptions,

static models of coronal loops are thermally unstable. The growth rate of the instability is of the order the coronal cooling time (20). The basic assumptions that we made for the equilibrium models were that gravity and all spatial variations in the loop area or heating rate are negligible. These are the most commonly used assumptions in calculating static models. An important question is: how sensitive are our results to these assumptions? McClymont and Craig (1981a,b,c) have considered the question of spatial variations in the heating rate. They find that these can act either to enhance or to damp instability. Lacking a model for the coronal heating process, nothing definitive can be stated on this issue; hence, we will not consider it further. We will discuss the effects of gravity and the area variation in a forthcoming paper. In general, the area variation acts to enhance the instability; however, we do not expect it to enhance the growth rates to values much beyond the ones here, since these are already of the order of the coronal cooling rate. Gravity, on the other hand, acts to damp the instability (e.g., Wragg and Priest 1982); hence, our results are certain to apply only for loops in which gravity can be neglected.

We can identify at least two possible physical situations in the solar corona where the effects of gravity should be small so that our results clearly apply. One is the case of loops sufficiently low lying, heights  $< 1000$  km, so that the loop height is smaller than any gravitational scale height in the loop. Another is the case of magnetic field lines that are concave in the corona, so that near the loop center the force of gravity is directed toward the center rather than away from it, as in the usual case. This is the type of magnetic geometry believed to be responsible for quiescent prominences. Our results imply that these two types of structures are naturally unstable without any special requirements on the

coronal heating process. We believe that the thermal instability discussed in this paper is responsible for the cool material that is often observed to occur in the corona.

Of course, in order to prove this statement, the nonlinear development of instability must be calculated. Clearly, the instability must not saturate at a low amplitude if it is to produce observational effects in the corona. Only the linear growth rates were considered in this paper; the nonlinear evaluation must be determined by numerical simulation. Numerical simulations of coronal loops have been performed by several authors (e.g., Craig, Robb, and Rollo 1982; Peres et al. 1982; Oran, Mariska, and Boris 1982). These simulations have not exhibited any significant evidence for thermal instability; however, to our knowledge no one has considered models in which the effects of gravity are negligible and the correct boundary conditions are employed at the loop base. Our results indicate that the instability should be present in such models. We intend to investigate the nonlinear stability of coronal loops in a future work.

#### Acknowledgments

The work at Stanford was supported by NASA Grants NGL 05-020-272 and NAGW-92 and ONR Contract N00014-85-K-0111 (formerly N00014-75-C-0673). The work at UCSD was supported by NASA Grant NSG-7406. Acknowledgment is made to the National Center for Atmospheric Research, which is sponsored by the National Science Foundation, for some of the computer time used in this research.

# References

- Antiochos, S. K. 1979, Ap. J. (Letters), 232, L125.
- Antiochos, S. K., and An, C.-H. 1985, Ap. J. (to be submitted).
- Athay, R. G. 1981, in Solar Phenomena in Stars and Stellar Systems  
(eds. R. M. Barnett and A. K. Dupree; Boston: D. Reidel), p. 173.
- Bonnett, R. M., and Dupree, A. K. 1980, Solar Phenomena in Stars and  
Stellar Systems (Dordrecht: D. Reidel).
- Chiuderi, C., Einaudi, G., and Torricelli-Ciamponi, G. 1981, Astron. Ap.,  
97, 27.
- Cox, D. P., and Tucker, W. H. 1969, Ap. J., 157, 1157.
- Craig, I. J. D., and McClymont, A. N. 1981, Nature, 294, 333.
- Craig, I. J. D., McClymont, A. N., and Underwood, J. H. 1978,
- Craig, I. J. D., Robb, T. D., and Rollo, M. D. 1982, Sol. Phys., 76, 331.
- Field, G. B. 1965, Ap. J., 142, 531.
- Habbal, S. R., and Rosner, R. 1979, Ap. J., 234, 1113.
- Hood, A. W., and Priest, E. R. 1980, Astron. Ap., 87, 126.
- McClymont, A. N., and Craig, I. J. D. 1981a, Univ. of Waikato Math. Res.  
Report No. 96.  
\_\_\_\_\_. 1981b, Univ. of Waikato Math. Res.  
Report No. 99.  
\_\_\_\_\_. 1981c, Univ. of Waikato Math. Res.  
Report No. 100.
- Morse, P. M., and Feshbach, H. 1953, Methods of Theoretical Physics  
(New York: McGraw-Hill), Ch. 6.
- Oran, E. S., Mariska, J. T., and Boris, J. P. 1982, Ap. J., 254, 349.
- Orrall, F. Q. 1981, Solar Active Regions (Boulder: Colo. Assoc. Univ.  
Press).

Peres, G., Rosner, R., Serio, S., and Vaiana, G. S. 1982, Ap. J., 252, 791.

Raymond, J. C., Cox, D. P., and Smith, B. W. 1976, Ap. J., 204, 290.

Richtmyer, R. D., and Morton, K. W. 1967, Difference Methods for Initial-Value Problems (2nd ed., New York: Interscience Publishers).

Rosner, R., Tucker, W. H., and Vaiana, G. S. 1978, Ap. J., 220, 643.

Shoub, E. C. 1983, Ap. J., 266, 339.

Spitzer, L. 1962, Physics of Fully Ionized Gases (New York: Wiley Interscience).

Vernazza, J. E., Avrett, E. H., and Loesser, R. 1981, Ap. J. Suppl., 45, 635.

Vesecky, J. F., Antiochos, S. K., and Underwood, J. H. 1979, Ap. J., 233, 987.

Wragg, M. A., and Priest, E. R. 1982, Astron. Ap., 113, 269.

### Figure Captions

- Figure 1 Plots of free-surface and rigid-wall pressure perturbation (Figure 1a) and mass flux perturbation (Figure 1b) for the highly simplified model described in the text. The free-surface results are indicated by solid curves and the rigid-wall one by broken curves; the two types of modes are distinguishable only near the base,  $s = L$ .
- Figure 2 The radiative loss coefficient of Raymond, Cox and Smith (1976) (broken line) and our analytic fit to it (solid line). The units in the figure are arbitrary.
- Figure 3 The free-surface (solid curve) and rigid-wall (broken curve) growth rates for a series of static models with varying base temperatures and/or varying base depths.
- Figure 4a Plot of lowest free-surface temperature perturbation ( $T_1/T_0$ ) and rigid-wall perturbation ( $T_1 P_0 / T_0 P_1$ ) for the equilibrium model with  $\delta = 5 \times 10^{-6}$  and a length  $L = 14.2 L_c$ . The free-surface mode is indicated by a solid curve, and the rigid-wall one by a broken curve; they are indistinguishable in the corona and transition region. The scale of the abscissa is  $\log (T_0)$  for  $0 \leq s \leq 2L_c$ , and  $s/L$  for  $2L_c < s \leq L$ .
- Figure 4b Same as in Figure 4a but for the equilibrium model with  $\delta = 10^{-3}$ , and with an abscissa of  $\log (T_0)$  for  $0 \leq s/L \leq .94$  and  $\log (s/L)$  for  $.94 \leq s/L < 1$ . Note that the rigid-wall amplitude is negative in the region  $s/L > .94$ .

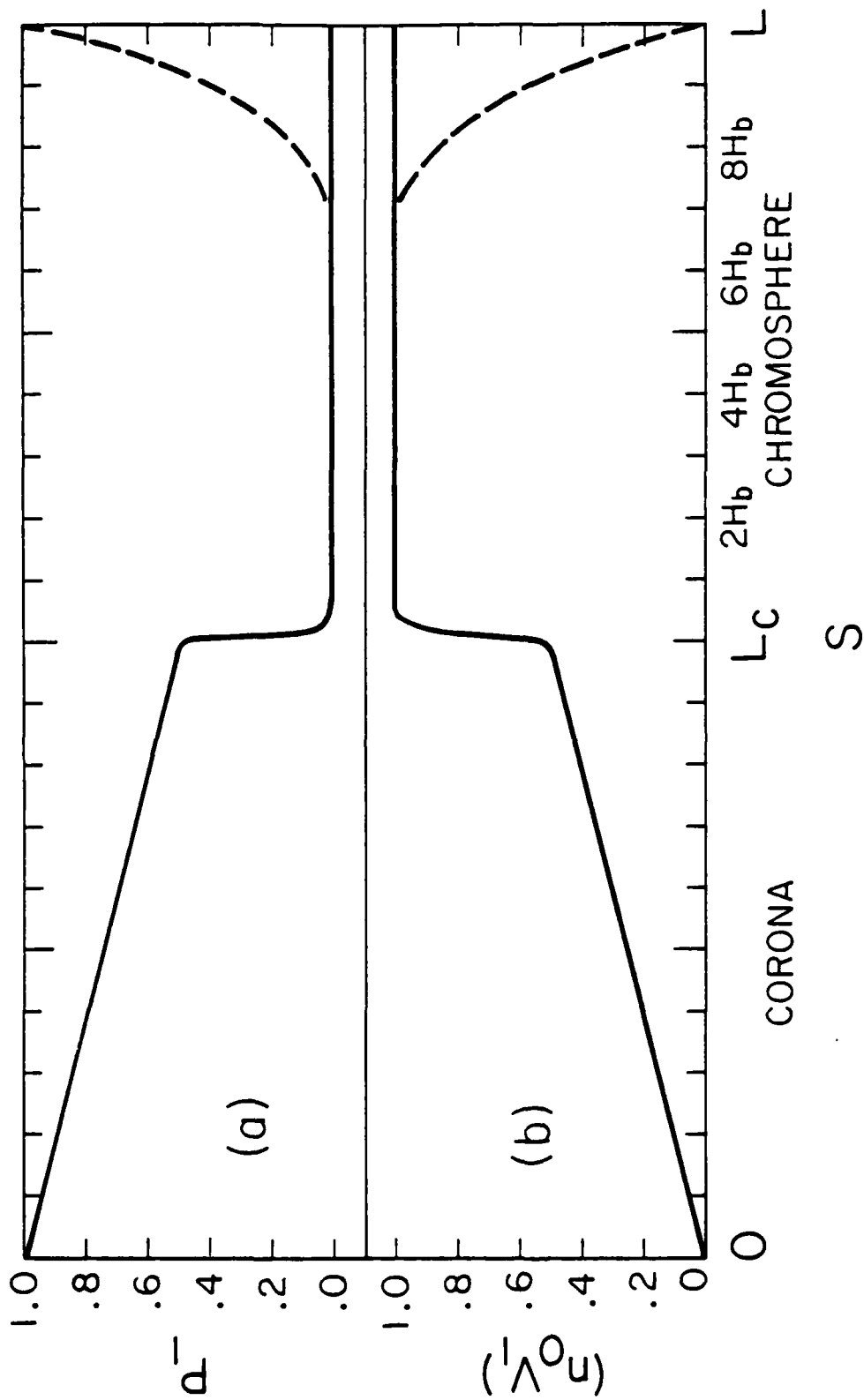


Figure 1



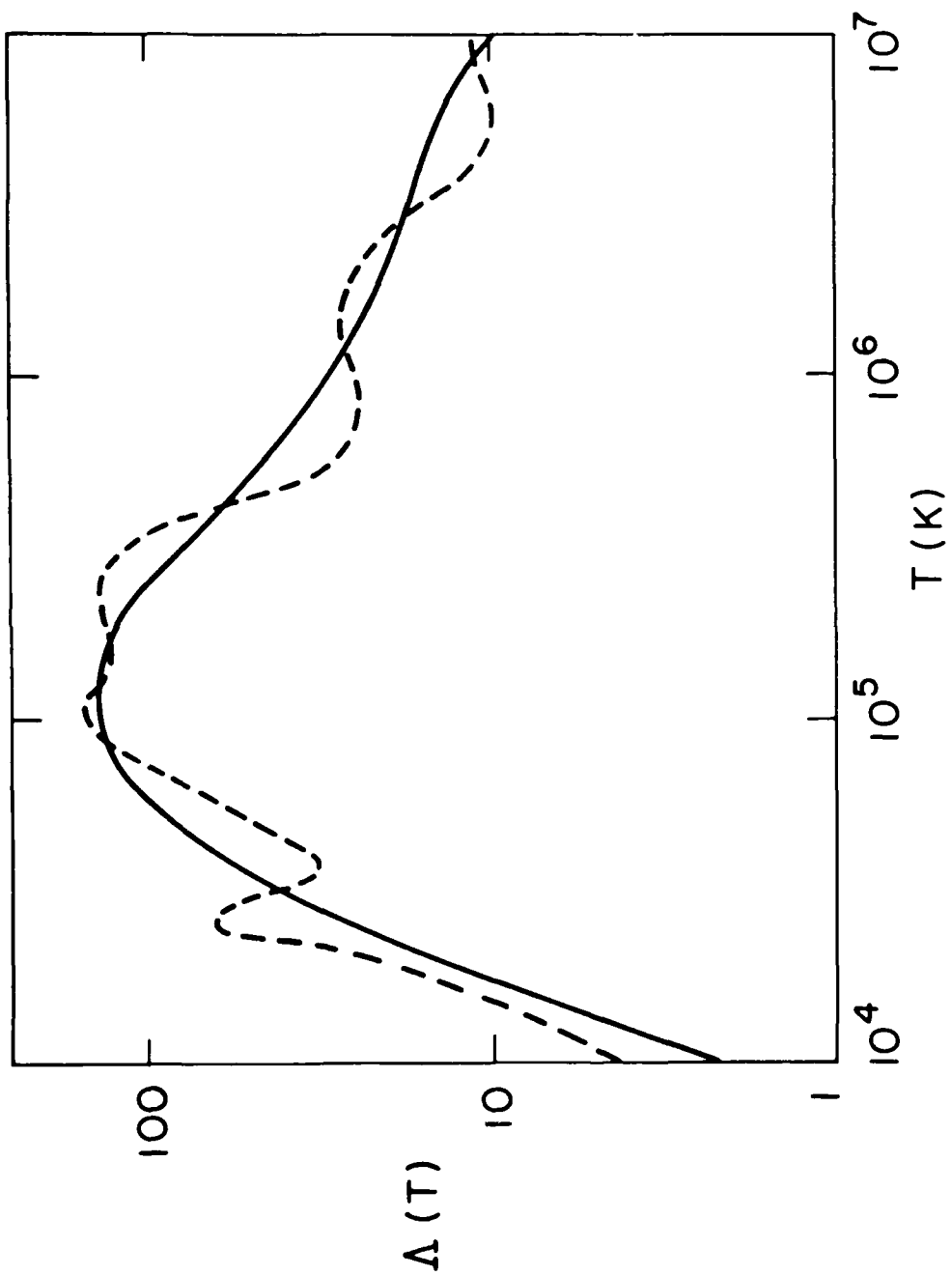


Figure 2

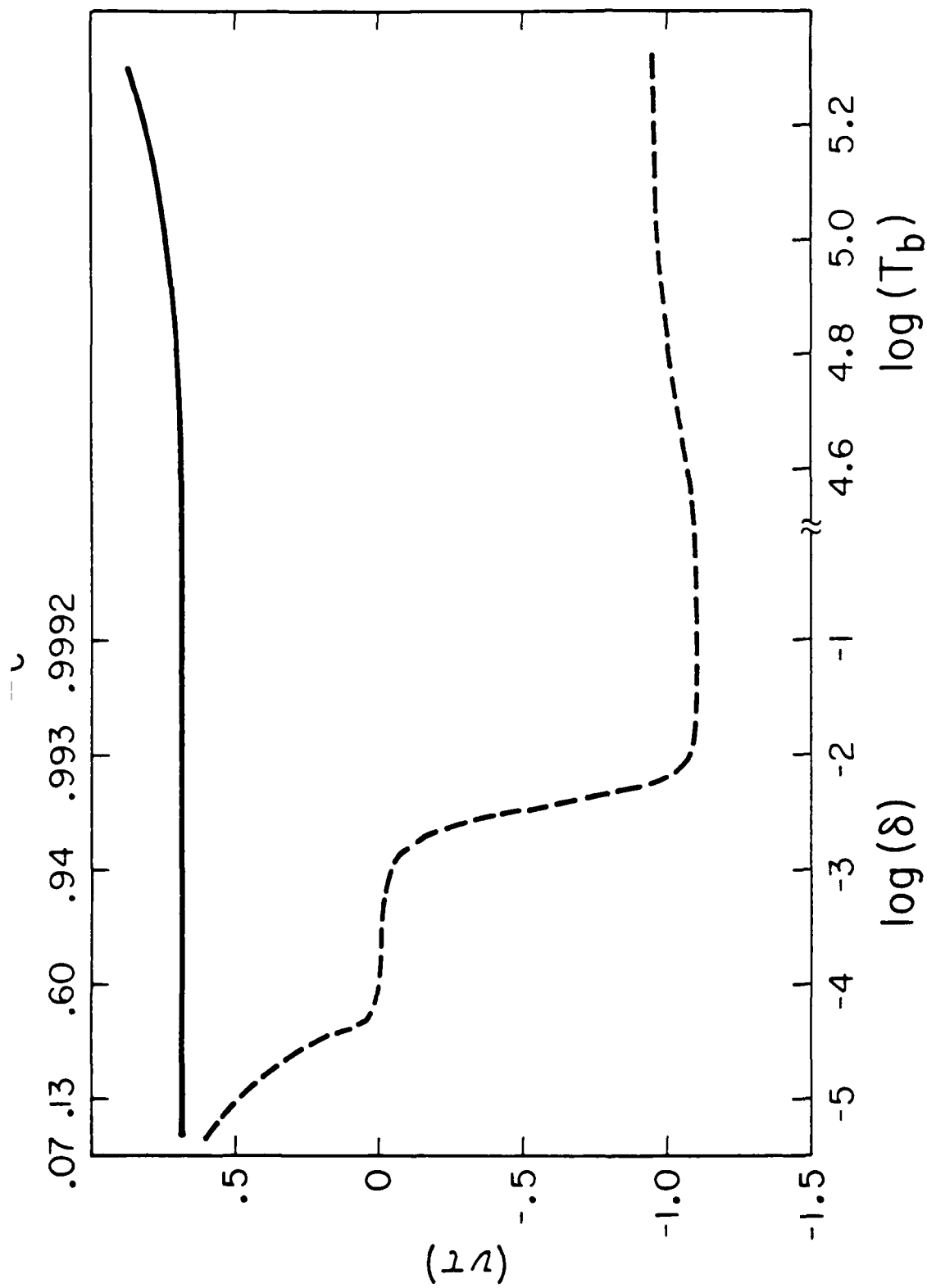


Figure 3

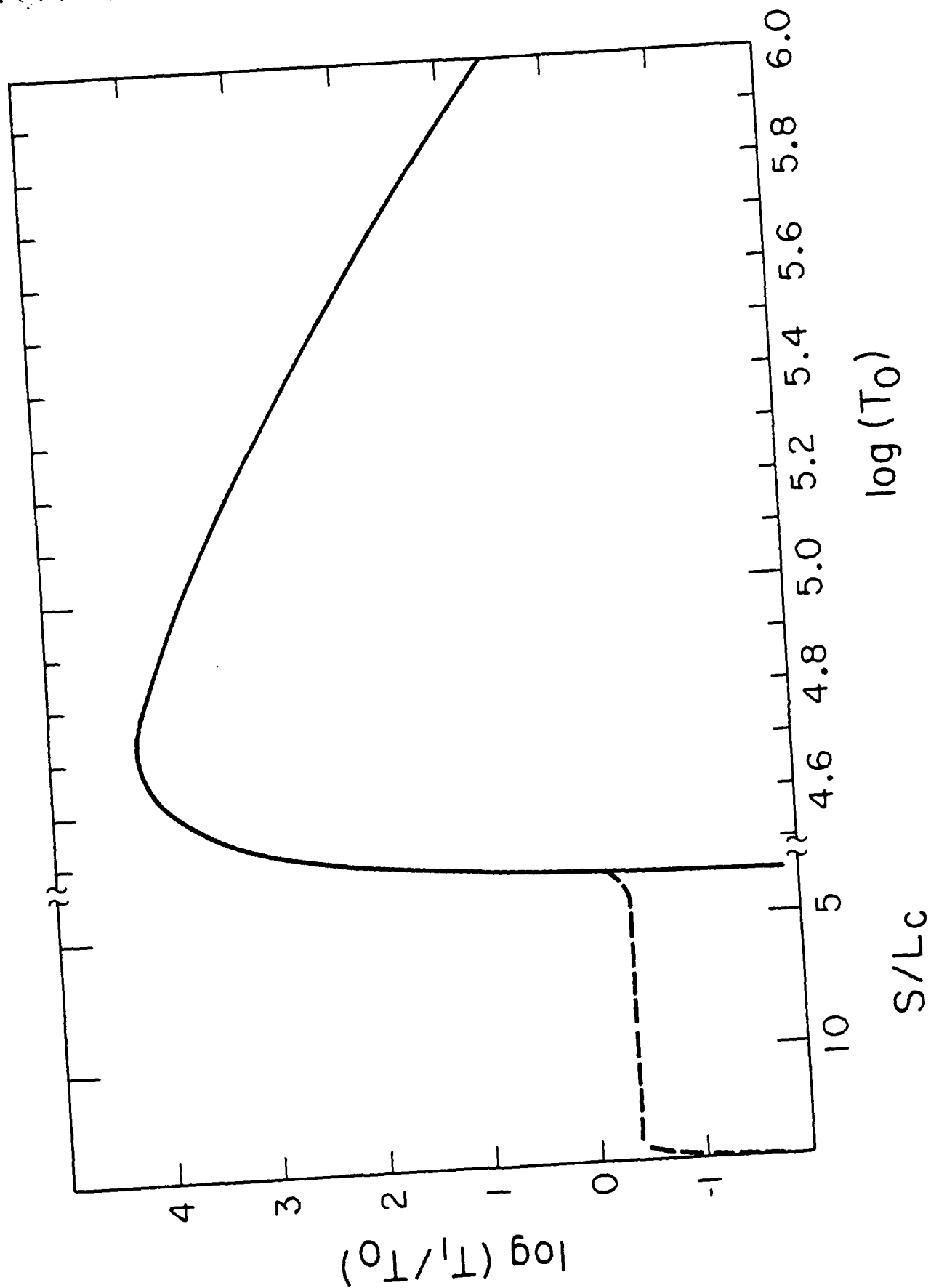


Figure 4a

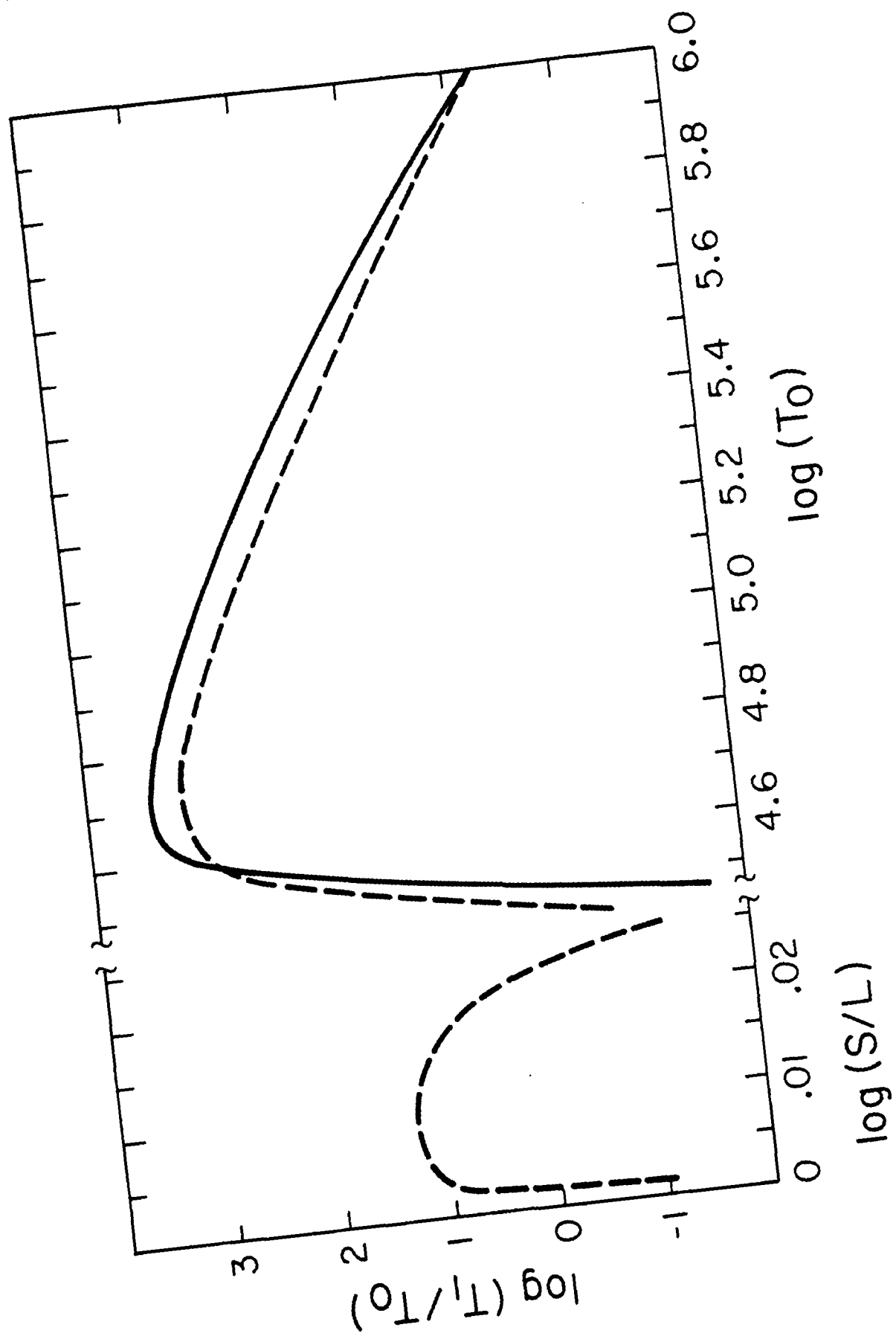


Figure 4b

**END**

**FILMED**

**6-85**

**DTIC**